

Viscosification in Polymer–Surfactant Mixtures at Low Temperatures

Neda Beheshti,[†] Anna-Lena Kjøniksen,^{†,§} Kaizheng Zhu,[†] Kenneth D. Knudsen,[‡] and Bo Nyström^{*,†}

Department of Chemistry, University of Oslo, P.O. Box 1033, Blindern, N-0315 Oslo, Norway, Department of Pharmaceutics, School of Pharmacy, University of Oslo, P.O. Box 1068, Blindern, N-0316 Oslo, Norway, and Department of Physics, Institute for Energy Technology, P.O. Box 40, N-2027 Kjeller, Norway

Received: January 13, 2010; Revised Manuscript Received: March 29, 2010

Interactions between the anionic surfactant sodium dodecyl sulfate (SDS) and hydroxyethylcellulose (HEC) or its hydrophobically modified analogue (HM-HEC) have been studied over an extended temperature region with the aid of turbidimetry, small-angle neutron scattering (SANS), and shear viscosimetry. Anomalous viscosity enhancements were observed for semidilute HEC/SDS and HM-HEC/SDS solutions at high SDS concentrations at temperatures far below the Krafft point for aqueous solutions of SDS. From the Arrhenius–Frenkel–Eyring (AFE) plots of the temperature dependence of the zero-shear viscosity, the activation energy of chain disengagement (ΔE_{vis}) was found to be on the order of 40 kJ mol^{−1} for the HEC/SDS mixtures, whereas for the HM-HEC/SDS system, much higher values of ΔE_{vis} (up to 141 kJ mol^{−1}) were reported, and the activation energy increased with an increasing level of SDS addition. Break points in the AFE plots were observed for both the HEC/SDS and HM-HEC/SDS systems at low temperatures and high SDS concentrations. Time evolutions of both the turbidity and the shear viscosity were monitored after quenching of the temperature from 25 to 1 °C. The turbidity results revealed in general a less pronounced transition for the HEC/SDS and HM-HEC/SDS systems than for the corresponding polymer-free SDS/water solutions. In the course of time, a significant viscosity enhancement was found for the HEC/SDS system at high levels of SDS addition, and a much stronger viscosification was observed for the HM-HEC/SDS system at the highest surfactant concentration. The overall results suggest that hydrated SDS aggregates act as cross-linkers of the network and generate the substantial viscosification of the systems at low temperature and high levels of SDS addition. For the HM-HEC/SDS system, further strengthening of the network occurs because of the contribution from hydrophobic interactions. The SANS data on HEC/SDS mixtures reveal that some structural reorganization takes place at low temperatures in the presence of high SDS concentrations, and this is ascribed to enhanced polymer–SDS interactions and the formation of clusters that strengthened the cross-links of the network.

Introduction

The synergism between hydrophobically modified water-soluble polymers (HMWSPs) and ionic surfactants has attracted significant interest in recent years in fundamental and applied research.^{1–4} This research field is driven by the importance of mixtures of amphiphilic polymers and ionic surfactants in a number of industrial applications, including detergents, paints, and pharmaceuticals.^{1–3} HMWSPs consist of a long hydrophilic chain to which small amounts of hydrophobic substituents are incorporated as pendant chains, blocks, or terminal groups. It is well-known^{2–4} that aqueous solutions of these polymers usually possess special dynamical and rheological properties, which arise from intra- or intermolecular associations of the hydrophobic groups. The physicochemical features of these polymers can be tuned by design, hydrophobicity, and interactions with cosolutes. In aqueous solutions of HMWSPs with an ionic surfactant, the structural and rheological behaviors of these systems are controlled by an intricate interplay between hydrophilic, hydrophobic, and electrostatic interactions.^{1–4} The addition of an ionic surfactant such as sodium dodecyl sulfate

(SDS) to an aqueous solution of a hydrophobically modified polymer usually leads to a viscosification of the solution at a moderate surfactant concentration, whereas at high levels of surfactant addition, the viscosity drops.⁴ The strong viscosity enhancement is ascribed^{2–4} to the formation of mixed polymer–surfactant micelles, whereas the viscosity drop at high levels of surfactant addition is attributed to the solubilization of the hydrophobic moieties. Most of the studies on the viscosification of aqueous mixtures of HMWSPs at different levels of surfactant addition have been carried out at ambient and elevated temperatures. However, very little is known about the effect of temperature on the viscosification at temperatures close to and below the Krafft point. Below this temperature, the solubility of the surfactant is very low and above this point the solubility can increase by orders of magnitude in a relatively narrow temperature region.³

In the present work, we report a novel and special viscosification effect in semidilute aqueous solutions of hydroxyethylcellulose (HEC) and its hydrophobically modified analogue (HM-HEC) in the presence of high concentrations of SDS at low temperatures. Although a noteworthy viscosification effect is detected for the HEC/SDS solution, a much stronger enhancement of the zero-shear viscosity (gel-like appearance) is observed for the corresponding HM-HEC/SDS sample at temperatures far below the Krafft temperature. The anomalous

* Corresponding author. E-mail: bo.nystrom@kjemi.uio.no.

[†] Department of Chemistry, University of Oslo.

[§] Department of Pharmacy, University of Oslo.

[‡] Institute for Energy Technology.

viscosification effect at high level of surfactant addition and low temperatures is a new finding, and to the best of our knowledge, this phenomenon has not been reported before. To gain further insight into the kinetics of the cross-linking process, the time evolution of the turbidity and the viscosity is monitored after a fast quenching to a low temperature below the Krafft point.

The aim of this study is to show that low temperatures, even below the Krafft point, can be used for an effective viscosity enhancement and to tune the strength of the network in polymer–surfactant mixtures. In the case of the HMWSP sample, it is demonstrated that a huge viscosification takes place over a long time after the temperature quenching. The hypothesis is that the polymer acts as nucleation sites for SDS, and the formed crystallites or clusters serve as cross-linkers of the network.

Experimental Section

In this study, a HEC sample with the commercial name Natrosol 250 GR (Lot No. A-0382), obtained from Hercules, Aqualon Division, was utilized as a reference and as the precursor for the synthesis of the hydrophobically modified analogue (HM-HEC). The degree of molar substitution of hydroxyethyl groups per repeating anhydroglucose unit of this cellulose derivative is 2.5 (given by the manufacturer), and this polymer has a quite hydrophilic character. The weight-average molecular weight ($M_w = 400\,000$) of this sample in dilute aqueous solution was determined by intensity light scattering⁵ at 25 °C. The anionic surfactant SDS was obtained from Fluka and was used as received.

The HM-HEC sample was synthesized according to a procedure described previously,⁶ and the details and characterization of the sample have been reported earlier by our group;⁷ therefore, only a brief summary is given here. After completion of the hydrophobization reactions, acetic acid neutralized the liquid reaction mixture, and the product was collected by filtration. The product was washed thoroughly with acetone and dried at 70 °C for 24 h under reduced pressure to remove the acetone. The chemical structure of the HM-HEC sample was ascertained by ¹H NMR (deuterated DMSO was used as a solvent) with a Bruker Avance DPX300 NMR spectrometer (Bruker Biospin, Fällanden, Switzerland) operating at 300.13 MHz at 298.2 K. The degree of hydrophobic substitution (glycidyl hexadecyl ether groups) of the sample was determined from the peak ratios between the anisomeric protons (4.9 ppm) and the methyl protons (0.8 ppm) of the glycidyl hexadecyl chain. The HM-HEC sample was found to contain 2 mol % C₁₆H₃₃ groups.

To remove salt and other low-molecular-weight impurities of HEC and HM-HEC, dilute solutions of each polymer were thoroughly dialyzed against Millipore water (7 days) and isolated by freeze-drying. Regenerated cellulose with a molecular weight cutoff of about 8000 (Spectrum Medical Industries) was utilized as the dialyzing membrane.

Samples were prepared in Millipore water by weighing the components, and the solutions were homogenized by stirring at room temperature for 1 day. All measurements were carried out in the semidilute regime at a fixed polymer concentration of 2.0 wt %. From viscosity measurements on dilute aqueous solutions of HM-HEC, the value of the intrinsic viscosity $[\eta]$ was found to be 4 wt %⁻¹, and the overlap concentration, c^* , estimated from $c^* = 1/[\eta]$, is 0.25 wt %, ⁸ which suggests that the considered concentration is well above c^* .

The turbidity measurements were conducted on an NK60-CPA cloud point analyzer from phase Technology, Richmond,

BC, Canada. A detailed description of the equipment and determination of turbidities has been given elsewhere.⁹ This apparatus utilizes a scanning diffusive technique to characterize phase changes of the sample with high sensitivity and accuracy. The light beam from an AlGaAs light source, operating at 654 nm, was focused on the measuring sample that was applied onto a specially designed glass plate that was coated with a thin metallic layer of very high reflectivity (mirror). Directly above the sample, an optical system with a light-scattering detector continuously monitored the scattered intensity signal (S) of the sample as it was subjected to prescribed temperature alterations. The relation between the signal and the turbidity (τ) is given by the following empirical relationship $\tau \text{ (cm}^{-1}\text{)} = 9.0 \times 10^{-9} S^{3.751}$.⁹

Small-angle neutron scattering (SANS) experiments were carried out at temperatures of 25 and 1 °C on the SANS installation at the JEEP II reactor, Kjeller, Norway. The wavelength used was 5.1 and 10.2 Å, with a resolution ($\Delta\lambda/\lambda$) of 10%. The length scale probed in SANS is controlled by the magnitude of the scattering vector, q , which is determined by the wavelength, λ , of the incident neutrons and the scattering angle, θ , through the expression $q = (4\pi/\lambda) \sin(\theta/2)$. The q range employed in the experiments was 0.008–0.25 Å⁻¹.

The samples were filled in 2 mm Hellma quartz cuvettes (with stoppers), which were placed onto a copper base for good thermal contact and mounted in the sample chamber. The space between the sample and the detector was evacuated to reduce air scattering. In addition, the sample chamber was evacuated to avoid condensation on the sample cell surfaces at the lowest temperature used. In all the SANS measurements, D₂O was used as a solvent instead of light water to obtain good contrast and low background for the neutron-scattering experiments.

Standard reductions of the scattering data, including transmission corrections, were conducted by incorporating data collected from empty cell, beam without cell, and blocked-beam backgrounds. The data were transformed to an absolute scale (coherent differential cross section ($d\Sigma/d\Omega$)) by calculating the normalized scattered intensity from direct beam measurements.

The steady shear viscosity experiments were carried out in a Paar-Physica MCR 300 or MCR 301 rheometer using a cone-and-plate geometry, with a cone angle of 1° and a diameter of 75 mm. This geometry was employed in all measurements. To prevent evaporation of the solvent, the free surface of the sample was always covered with a thin layer of low viscosity silicone oil (the values of the viscosity for the samples considered in this investigation are virtually not affected by this layer). The measuring device is equipped with a temperature unit (Peltier plate) that gives an effective temperature control (± 0.05 °C) over an extended time for the temperatures studied in this work. The experimental accuracy is within the size of the symbols in the Figures.

Results and Discussion

It is generally known^{2–4} that addition of a surfactant to a semidilute solution of a hydrophobically modified polymer at ambient temperature usually leads to viscosification at low or moderate surfactant concentrations, whereas at high level of surfactant addition, the viscosity drops because of solubilization of hydrophobic moieties. For an ionic surfactant dissolved in water, the system can form different phases,¹⁰ depending on the surfactant concentration and temperature. The following phases can be visualized: (1) a surfactant solution of unimers, (2) unimers together with suspended micelles, and (3) unimers together with crystalline hydrated surfactant. This scenario leads

to two critical concentrations of the surfactant; namely, the surfactant solubility concentration, above which the surfactant forms a hydrated solid at temperatures below the Krafft point, T_K ; and the critical micelle concentration (CMC), above which the surfactant forms micelles at temperatures above T_K . The general opinion^{10–14} is that at temperatures below T_K , the solubility of an anionic surfactant, such as SDS is too low to form micelles in the aqueous phase. The picture that emerges is that below T_K , noncrystallized surfactant unimers coexist with the crystalline hydrated surfactant species.¹² The Krafft point is the temperature (more precisely, narrow temperature interval) above which the solubility of a surfactant rises sharply, and at this temperature, the solubility of the surfactant becomes equal to the CMC.¹⁵ The reported values^{16–18} of T_K for SDS in water are in the interval 12 ± 4 °C and the CMC determined at ambient temperature is 8.1 mM.¹⁹ This broad range of values of T_K may indicate an experimental difficulty in determining T_K or point to the intrinsically indefinite nature of T_K . It has been claimed²⁰ that the Krafft temperature is not a single point but a diffuse temperature region.

In an aqueous mixture of a polymer and a surfactant, a more intricate scenario evolves, especially at low temperatures. At ambient temperature, it is usually assumed that the binding of surfactant to the polymer occurs at a critical aggregation concentration (CAC), above which the surfactant will associate cooperatively and bring polymer chains together in the form of mixed polymer–surfactant micelles.^{3,4} The CAC is typically lower than CMC for the corresponding water–surfactant system. However, in the case when the hydrophobic tails are attached to the polymer backbone (as for the HM-HEC), it has been reported^{21,22} that the value of CAC is very low or nonexistent; that is, the surfactant is adsorbed in a noncooperative way as soon some surfactant molecules are present. At low or moderate surfactant concentrations, the network chains are tightly connected to each other through micellar-type cross-links between the polymer chains and surfactant (the surfactant works as a cross-linking agent), whereas in an excess of surfactant, many junctions are solubilized, yielding a loosely bound network.

At temperatures below T_K , the behavior of the polymer–surfactant mixtures is more complex. It is possible that the solid hydrates act as cross-linkers for the polymer chains or that the surfactant molecules can form junctions together with the polymer chains. It is plausible that the polymer chains act as nucleation sites for the growth of the SDS crystallites. Another phenomenon that should be considered is the ability of a water-soluble polymer to expand the solubility domain of a surfactant. It has previously been reported^{1,23} that the polymer polyvinylpyrrolidone can reduce the T_K of sodium hexadecyl sulfate by approximately 10 °C, an effect that gives rise to a lowering of the monomer concentration required for aggregation in the presence of this polymer. Furthermore, it has been found²⁴ that T_K is significantly reduced in mixtures of poly(amidoamine) dendrimers and SDS.

Below, we will discuss the influence of temperature on the shear viscosity in the framework of these approaches, and subsequently, the time evolution of the turbidity and shear viscosity will be presented when the samples are quenched from 25 to 1 °C. The idea is to gain insight into the time window for these processes when the polymer network is strengthened in the course of time. In the last part of this section, SANS results will be presented and discussed to examine how the structure of the polymer network is changed upon cooling at high levels of SDS addition.

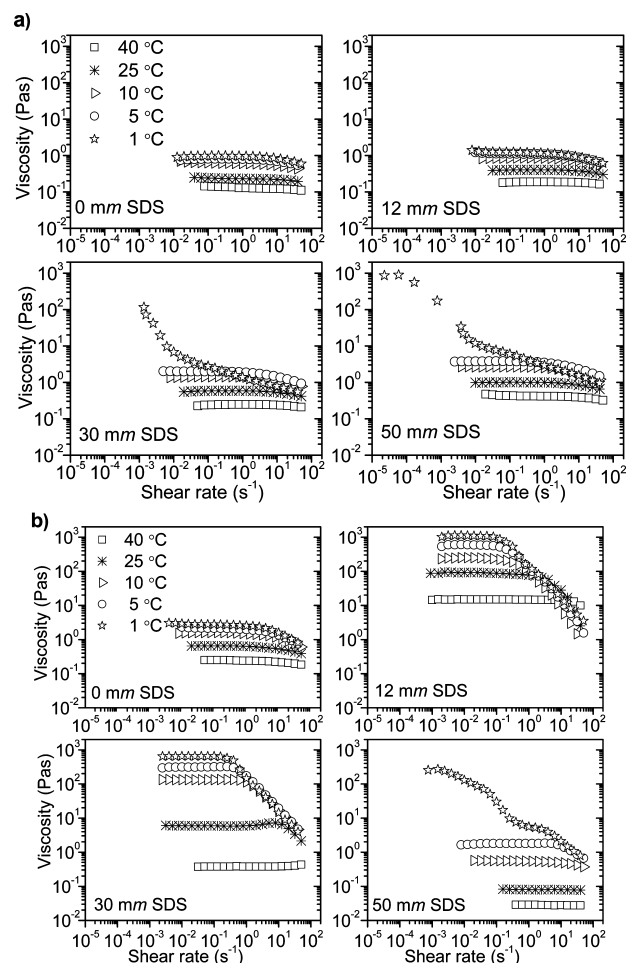


Figure 1. Shear rate dependencies of the viscosity for 2 wt % solutions of HEC (a) and HM-HEC (b) at the temperatures and SDS concentrations indicated.

Shear Viscosity and the Relative Zero-Shear Viscosity.

Figure 1 shows the shear rate dependence of the viscosity at various temperatures for 2 wt % solutions of HEC and of HM-HEC in the presence of different amounts of SDS. At each temperature of measurement, the solutions were allowed to equilibrate for 1 h prior to the next viscosity run. For the HEC solutions without SDS and with 12 mM SDS, Newtonian behavior is observed at low shear rates for all temperatures, and only a modest shear-thinning effect is detected at high shear rates (Figure 1a). A more complex viscosity feature is found for the HEC samples with 30 and 50 mM SDS at the lowest temperature. In this case, a strong upturn of the viscosity is observed at low shear rates, and this suggests the evolution of hydrates or clusters that act as cross-linkers of the polymer chains. The observation of marked shear-thinning already at low shear rates indicates that the junctions are rather weak.

The shear rate dependence of the viscosity for 2 wt % solutions of HM-HEC in the presence of different levels of SDS and various temperatures (Figure 1b) reveals Newtonian behavior at low shear rates for all samples and temperatures, and pronounced shear-thinning is found for the associative networks that exhibit marked viscosity enhancement. At the highest surfactant concentration, a strong upturn of the viscosity is registered at low shear rates at the lowest temperature. This illustrates again the anomalous viscosity behavior observed at high SDS concentration and low temperature. The progressive decrease in viscosity as the shear rate rises is attributed to the breakdown of the network junctions; that is, the rate of network

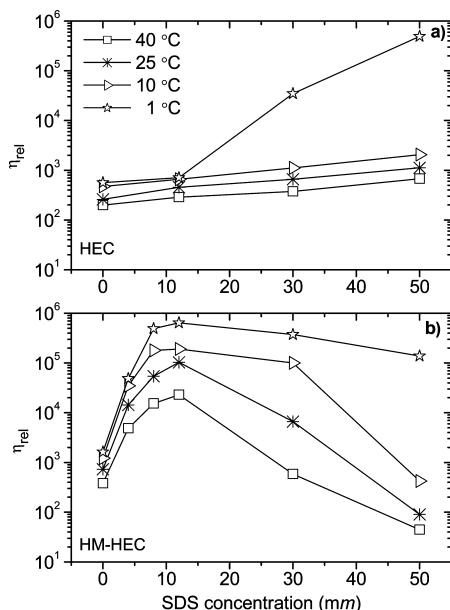


Figure 2. Surfactant concentration dependencies of the relative zero-shear viscosity for 2 wt % solutions of HEC and HM-HEC at the temperatures indicated.

disruption exceeds the rate at which cross-links are reformed. At all surfactant concentrations, a low temperature promotes a strong augmentation of the viscosity.

The solvent viscosity is affected by temperature, and to take into account trivial changes of the solvent viscosity with temperature, the zero-shear viscosity results are presented in terms of the relative viscosity η_{rel} ($\eta_{\text{rel}} \equiv \eta/\eta_{\text{solvent}}$, where η_{solvent} is the viscosity of water or the viscosities of the water–SDS mixtures). In Figure 2, the effects of temperature and the addition of surfactant on the relative zero-shear viscosity are depicted for 2 wt % solutions of HEC and HM-HEC. For the HEC/SDS system (Figure 2a), only a moderate increase in η_{rel} with increasing SDS concentration takes place at temperatures above 1 °C. This trend is ascribed to poorer thermodynamic conditions for the polymer upon addition of the ionic surfactant, which can act as a salt and cause a salting-out effect, leading to enhanced associations within the polymer network and thereby inducing a rise in the viscosity. The fact that the value of the relative viscosity at a given SDS concentration decreases with rising temperature is associated with enhanced mobility of the polymer chains at an elevated temperature, leading to loosening of the polymer network. The strong upturn of the relative viscosity at the higher two levels of surfactant addition for the HEC/SDS system at 1 °C can be related to the formation of hydrates or clusters of surfactant molecules, which act as cross-links and thereby strengthen the network. Since HEC is hydrophilic, it is unlikely that hydrophobic interaction between the polymer and the surfactant may play an essential role in the strengthening of the network at low temperatures. In this context, it is interesting to note recent rheological studies on semidilute aqueous solutions of alginate²⁵ and HEC²⁶ in the presence of β -cyclodextrin. For both systems, a marked viscosity enhancement was observed at low temperatures and high β -cyclodextrin concentrations. It is well-established^{27,28} that β -cyclodextrin develops crystallites at low temperatures, and it was argued that polymer chains were cross-linked through the formation of β -cyclodextrin clusters or crystallites.

The viscosity results for mixtures of HM-HEC/SDS at different temperatures (Figure 2b) disclose that the relative

viscosity passes through a more or less pronounced maximum (located at ~ 10 mm SDS for all temperatures). At low and moderate surfactant concentrations up to the viscosity maximum, the hypothesis is^{2–4} that hydrophobic tails of the polymer and hydrophobes on the surfactant aggregate into mixed micelles that act as cross-link junctions in the evolution of the associative network. At the viscosity maximum, the number of mixed-micelle intermolecular links is optimal, and the lifetime of the hydrophobes inside them has reached its optimum. At higher levels of SDS addition, a progressive solubilization of the hydrophobic moieties occurs, and this leads to a reduction of the number of efficient cross-links, and the network becomes gradually weaker (the viscosity decreases).

In this process, a changeover from polymer-dominated to surfactant dominated micelles takes place.^{29–32} An inspection of the data shows that the maximum of the viscosity curve becomes more centered at lower values when the temperature is altered from 1 to 40 °C. This effect is attributed to enhanced mobility of the polymer chains at elevated temperature, leading to loosening of the associative network with an accompanying viscosity drop. The dramatic effect of temperature on the relative viscosity at the highest SDS addition (50 mm) can be rationalized in the following way: At the lowest temperature (1 °C), only a modest decrease of η_{rel} with increasing surfactant addition is observed after the viscosity maximum. This is attributed to the low solubility of the surfactant at this temperature, and even at a high level of SDS addition, the fraction of polymer-dominated micelles is high, and the effect of solubilization of the hydrophobic moieties as well as the chain mobility is low at a low temperature. In addition, it is likely that cross-linking of the polymer network via the formation of hydrate complexes at high levels of surfactant addition may contribute to this behavior.

Temperature Dependence of the Viscosity and Activation Energy. To take a closer look at the temperature effect of the zero shear viscosity and to gain a more detailed insight into the cross-linking mechanism, the temperature dependence of η_0 is analyzed by the Arrhenius–Frenkel–Eyring relation³³ in the logarithmic form as $\log \eta_0 = \log A + \Delta E_{\text{vis}}/2.303RT$ (see Figure 3), where A is the pre-exponential factor, ΔE_{vis} is the free activation energy for viscous flow, η_0 is the zero shear viscosity at absolute temperature T , and R is the gas constant. Most of the HEC/SDS and HM-HEC/SDS mixtures exhibit a good linear relationship between $\log \eta_0$ and $1/T$ over an extended temperature region, in agreement with the kinetic rate theory of flow as represented by the expression above. However, there are important deviations from linearity observed for the HEC and HM-HEC solutions at high surfactant concentrations and low temperatures that we will return to later. The observed linearity of $\log \eta_0$ versus $1/T$ relationships of these HEC/SDS and HM-HEC/SDS mixtures indicates that within the considered temperature interval, their apparent activation energy of flow (ΔE_{vis}) is constant and independent of temperature. The effects of surfactant addition on ΔE_{vis} for solutions of HEC and HM-HEC are given in the inset of Figure 3a. For the HEC/SDS system, there is only a slight change in the value with increasing surfactant concentration, suggesting that the polymer–surfactant interactions are weak. These values are in the same range (20–40 kJ/mol) as reported^{34–37} for other polysaccharides.

For the HM-HEC/SDS system, the value of ΔE_{vis} increases markedly with increasing levels of SDS addition, reflecting the formation of a large number of long-lived, intersegmental clusters between hydrophobic entities of the polymer backbone and surfactant micelles. Substantially higher values of ΔE_{vis} are

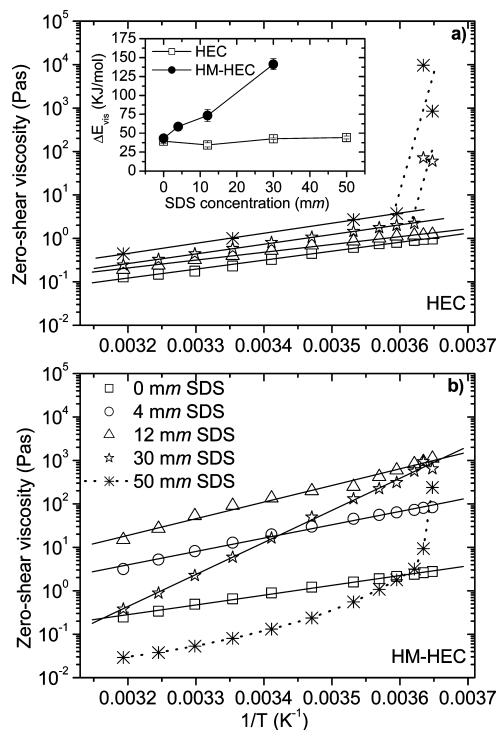


Figure 3. Temperature dependencies of the zero shear viscosity for 2 wt % solutions of HEC and HM-HEC at the surfactant concentrations indicated. ΔE_{vis} is calculated from the solid fitted lines and is displayed in the inset plot.

usually reported^{38–41} for associating polymers. In a previous investigation³⁹ on the temperature dependence of the zero shear viscosity in aqueous mixtures of a hydrophobically modified, alkali-soluble emulsion polymer in the presence of a nonionic surfactant, a rather complex picture emerged. In the absence of surfactant, an Arrhenius type of relation yielded an activation energy of 50 kJ/mol. In the presence of 0.25 mM surfactant, an increase in the activation energy of about 10% was found, and this was attributed to augmentation of the hydrophobic junctions by the surfactant molecules. At surfactant concentrations in the range 1–10 mM, the Arrhenius type of plot disclosed two distinct regions, yielding activation energies of 30 kJ/mol at temperatures $T < 25^\circ\text{C}$ and 75 kJ/mol at $T > 25^\circ\text{C}$. The behavior at low temperatures was ascribed to the formation of spherical micellar aggregates, whereas at high temperatures, they suggested a large bilayered structure formed by the polymer–surfactant aggregates. This type of complexity was not observed in the present work.

The good linearity with no breaks in the plots of $\log \eta_0$ versus $1/T$ for the systems discussed above indicates that there is only one type of mechanism responsible for the disengagement of chains over the considered temperature region at a given condition. However, for the HEC/SDS systems with 30 and 50 mM SDS concentration and for the HM-HEC/SDS system with 50 mM SDS, significant deviations from the Arrhenius–Frenkel–Eyring behavior are displayed (Figure 3). For the HEC/SDS mixtures, breaks in the plots are detected at low temperatures, and for the HM-HEC/SDS(50 mM) solution, a strong upturn of η_0 is observed at low temperatures (see Figure 3b). In this case, a progressive deviation from linearity is found over a broad temperature range. These phenomena are ascribed to a different mechanism for the cross-linking of the associative network at low temperatures and high SDS concentrations. These anomalies can lend support to the hypothesis above that hydrated SDS clusters act as cross-linkers, and the mechanism

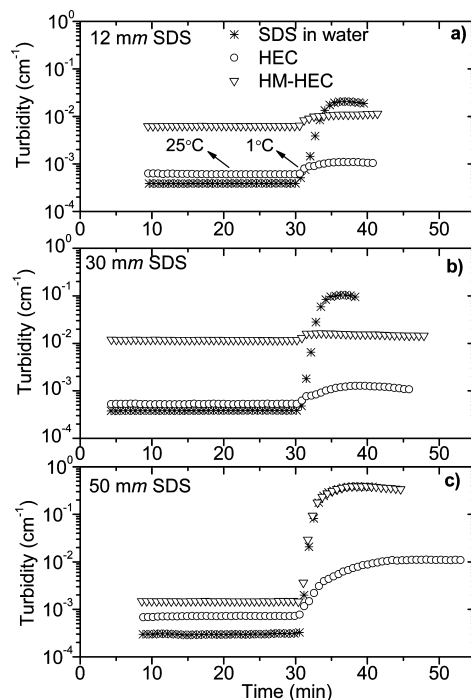


Figure 4. Plot of the turbidity as a function of time for SDS/water solutions and for 2 wt % solutions of HEC and HM-HEC in the presence of various levels of added SDS. The samples were equilibrated at 25°C for 30 min prior to a fast temperature quenching to 1°C , and the time evolution of the turbidity was monitored.

of this process is expected to be fundamentally different from the formation of mixed polymer–surfactant micelles. Since deviations from linearity are observed for both the HEC/SDS and HM-HEC/SDS systems, it is difficult to imagine that the formation of mixed polymer–surfactant micelles is the only process responsible for this feature.

Temperature Quenching and Time Evolution of the Turbidity and the Viscosity. The formation and growth of crystal-like clusters are usually governed by a kinetically rather complex process. To gain a more detailed insight into the kinetics, we have rapidly quenched the samples from 25 to 1°C and monitored the time evolution of the turbidity and the shear viscosity. In Figure 4, the time evolution of the turbidity for the systems SDS/water, HEC/SDS, and HM-HEC/SDS at different levels of SDS addition is depicted. During the first 30 min, the samples are allowed to equilibrate at 25°C before the solutions are quickly quenched to 1°C and the turbidity is recorded in the course of time. Before quenching, the turbidity is constant, and higher values of τ are found for the mixtures with HM-HEC at all SDS concentrations. For all the SDS/water solutions, very marked transitions of τ with increasing SDS concentration are observed during a short period of time, and the turbidity flattens out at longer times. Since the quenching temperature is far below the Krafft point of SDS, the pronounced increase in τ reflects the formation of clusters and incipient precipitation; this tendency is stronger as the surfactant concentration increases.

For the HEC/SDS and HM-HEC/SDS solutions, a much weaker turbidity transition is registered, except for the HM-HEC/SDS mixture with the highest surfactant concentration (50 mM), for which the turbidity curve coincides with that for the SDS/water system (see Figure 4c). The latter finding suggests that intense interactions between the surfactant and the hydrophobic moieties of the polymer lead to the formation of large association structures. An alternative speculation about the

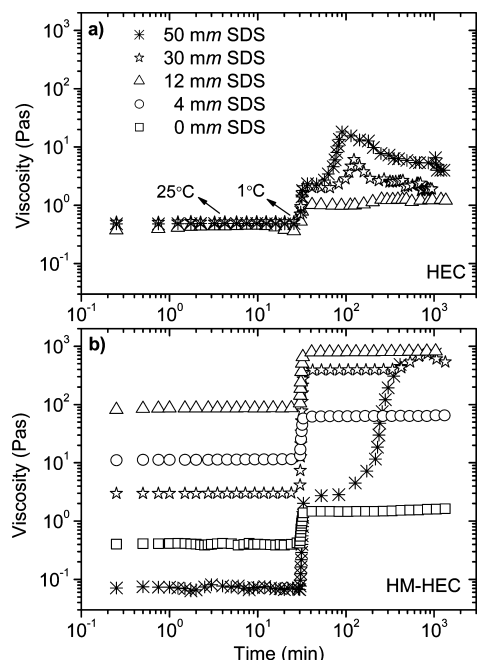


Figure 5. Plot of the shear viscosity (constant shear rate of 0.1 s^{-1}) as a function of time for 2 wt % solutions of HEC and HM-HEC in the presence of various levels of added SDS. The samples were equilibrated at 25 °C for 30 min prior to a fast temperature quenching to 1 °C, and the time evolution of the shear viscosity was monitored.

massive turbidity transition for the HM-HEC/SDS (50 mm) system can be that only a small amount of the surfactant is consumed in the formation of the junction zones; therefore, many crystallites of SDS are developed in the bulk as for the SDS/water pair without polymer. As will be discussed below, the substantial turbidity alteration is accompanied by high values of the viscosity in the course of time. The weaker turbidity transitions found for the other polymer–surfactant pairs indicate that the surfactant molecules are adsorbed and distributed over the polymer networks, and the tendency of the surfactant to form crystalline hydrated SDS aggregates in the bulk is suppressed. This may indicate that the polymers have the ability to expand the solubility range of the surfactant and thereby reduce the Krafft point of SDS in a way similar to what has been found for other polymers.²⁴

Figure 5 shows the corresponding time evolution of the shear viscosity (at a low fixed shear rate of 0.1 s^{-1}) for 2 wt % solutions of HEC and HM-HEC in the presence of various levels of SDS addition. In the same way as for the turbidity measurements, the samples are equilibrated at 25 °C for 30 min prior to a fast temperature quenching to 1 °C; thereafter, the development of the shear viscosity is probed over a long time.

Let us first consider the results for the HEC/SDS system. The quenching leads under all conditions to a quick jump of the viscosity, and in the absence of surfactant or at low SDS concentrations, the viscosity is constant in the course of time. However, even at a SDS concentration of 12 mm, a “hump” in the viscosity can be discerned at long times. At the higher two SDS concentrations, a pronounced peak (the maximum of the peak is located after ~ 100 min) is observed in the viscosity curve at long times, and the viscosity enhancement is stronger for the highest surfactant concentration. The decrease in the viscosity at very long times can probably be attributed to shear flow-induced breaking up of junction zones. The hypothesis that the cross-links are weak is supported by the strong shear rate

dependence of the viscosity at low shear rates for these levels of SDS addition (cf. Figure 1a). It should be noted that for these surfactant concentrations (30 and 50 mm), distinctive break points in the Arrhenius–Frenkel–Eyring plots were observed (see Figure 3a). This supports the conjecture that another mechanism is responsible for the viscosification at low temperatures and high levels of SDS addition.

For the HM-HEC/SDS system (Figure 5b), a very strong viscosification (more than two decades) is observed only for the sample with the highest level (50 mm) of surfactant addition, and the lower surfactant concentrations only exhibit a smaller viscosity change. The viscosity continues to grow for about 8 h and then it levels off. The viscosification effect is much larger for the HM-HEC/SDS than for the HEC/SDS system because both hydrated clusters and hydrophobic interactions contribute to the strength of the network. Actually, if a tube with a HM-HEC/SDS (50 mm) solution is cooled down to 1 °C and kept there for a long time, the tube can be turned upside-down, and no flow is detected, suggesting the formation of a gel. The general picture that emerges is that hydrates are formed at high surfactant concentration and low temperature, and these clusters serve as cross-linkers of the polymer network. It is to be expected that the kinetics of such a process is slow, and this is reflected in the time-dependent viscosification.

Small-Angle Neutron Scattering. The SANS technique can be utilized to probe “local” structural features of polymer–surfactant complexes at different conditions; for example, the effects of temperature and the level of surfactant addition. To gain more insight into the morphology of SDS species in aqueous solution at different temperatures, the scattered intensity profiles of 30 mm SDS in D_2O at 25 and 1 °C are displayed in Figure 6a. In solutions of 30 mm SDS, a broad interaction peak appears at 25 °C in the integrated pattern, corresponding to the distance correlation introduced by the interaction between the charged micelles. The q value for the center of this peak, $\sim 0.06 \text{ \AA}^{-1}$, corresponds to an average distance between the micelles of $2\pi/0.06 \text{ \AA}^{-1}$; that is, $\sim 105 \text{ \AA}$.

Interestingly, at low temperature (1 °C), the overall scattering becomes very weak, and the interaction peak that was dominant at 25 °C now disappears completely. However, two well-defined diffraction spots appear in the image. These can be due only to regularly packed structures; that is, crystallites that happen to be oriented in a position such that they satisfy the Bragg condition at the wavelength used (5.1 Å). When the pattern is integrated (giving scattered intensity vs q), these peaks appear as a small bump in the pattern having its center at approximately $q = 0.2 \text{ \AA}^{-1}$. This is equivalent to a repeating distance of $2\pi/0.2 \text{ \AA}^{-1}$, that is, $\sim 30 \text{ \AA}$. Incidentally, this corresponds well to the c -axis in the unit cell of crystallized, hydrated SDS, as reported in an earlier study.⁴² Thus, it is clear that SDS is able to crystallize in our systems and that one can expect micro-/nanocrystals to be present in the HEC/HM-HEC samples at low temperatures (1 °C). However, the extent of interaction between SDS (when being in its crystalline form) and the polymer chains is difficult to quantify in detail.

Figure 6b shows the variation of the SANS scattering intensity as a function of q (log–log plot) for HEC (2 wt %)/SDS mixtures and HEC without SDS at 25 and 1 °C. For the HEC solution and in the presence of 10 mm SDS, the corresponding scattered intensity curves are flat, and the intensity is quite low; virtually no temperature effect is observed. At an SDS concentration of 30 mm, an interaction peak (bump around $q = 0.06 \text{ \AA}^{-1}$) is developed in the intermediate q region, and a temperature effect can be discerned. It is interesting to note that even at 1

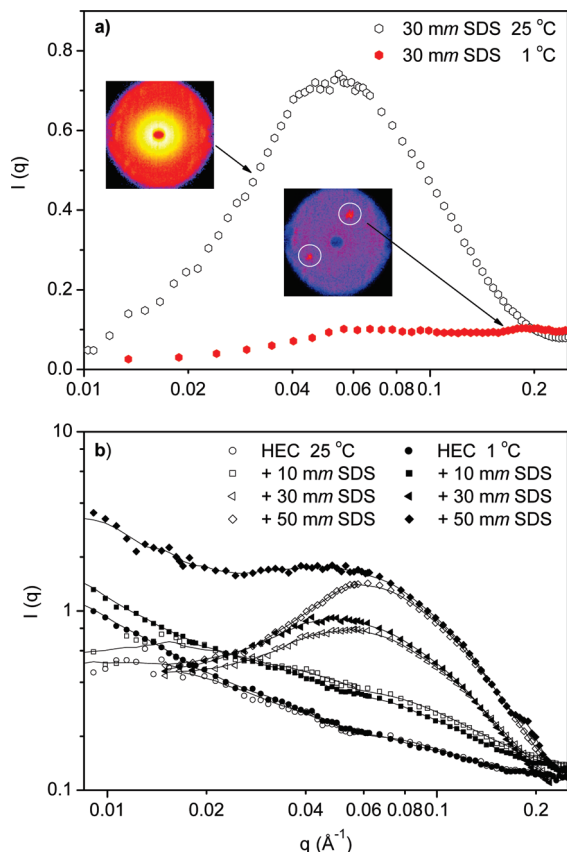


Figure 6. SANS scattered intensity profile as a function of scattering vector for 30 mM SDS in D₂O (a), and for 2 wt % solutions of HEC with and without SDS (b) at the temperatures and SDS concentrations indicated.

°C, a strong peak is visible, and this result is in contrast to the behavior observed at 30 mM SDS in the absence of polymer (cf. Figure 6a). Thus, the polymer clearly has a stabilizing effect on this system.

At low temperature, the presence of the polymer hinders the formation of *large* SDS crystals that would otherwise precipitate out of the solution. This behavior does not mean that SDS crystals cannot form at low temperature with polymer present, but to the extent that they exist, they must generally be small individual microcrystals or mixed polymer/SDS microcrystals/clusters. In the presence of 50 mM SDS at 25 °C, a marked peak is found at intermediate q values. An inspection of these curves reveals that the position of the peak moves to higher q values when the SDS concentration is increased from 30 to 50 mM. This is reasonable, since it corresponds to an expected reduction in intermicellar distance (the reduction can here be estimated to ~ 10 Å).

The most conspicuous feature of the scattered intensity profile at 50 mM SDS is that at low temperature, where the correlation peak diminishes and a strong upturn of the scattered intensity is observed at low q values. This indicates that some structural reorganization takes place upon cooling at this SDS concentration, and it could be a signature of the increased polymer–SDS interaction (cluster formation). This may suggest that a heterogeneous network is formed because of the special character of the cluster junctions; however, the exact nature of the change is not easy to identify from these data.

Conclusions and Summary

In this work, some novel features at low temperatures are reported for semidilute aqueous solutions of a hydrophilic

polymer (HEC) and its hydrophobically modified counterpart (HM-HEC) in the presence of the anionic surfactant SDS. The main findings from this study can be summarized in the following way: (i) An anomalous viscosity enhancement is observed for the HEC/SDS system at a low temperature and high SDS concentrations. For the HM-HEC/SDS solutions, a marked drop in the relative zero shear viscosity is found at elevated temperature in the presence of a large amount of SDS, whereas only a modest decrease in η_{rel} is detected at a low temperature.

(ii) The temperature dependence of the zero-shear viscosity can be described by the Arrhenius–Frenkel–Eyring (AFE) model, and the calculated activation energy of chain disengagement (ΔE_{vis}) is on the order of 40 kJ mol^{−1} for the HEC/SDS system, whereas for the HM-HEC/SDS system, the value of ΔE_{vis} increases with increasing SDS concentration (from 43 to 141 kJ mol^{−1}). Deviations from linearity in the AFE plots are observed for both the HEC/SDS and HM-HEC/SDS systems at low temperatures and high levels of SDS addition.

(iii) Time evolutions of the turbidity and the viscosity were monitored after a fast temperature quenching from 25 to 1 °C. The turbidity results show in general that the temperature-induced transition of the turbidity for the HEC/SDS and HM-HEC/SDS systems is less pronounced than for the corresponding polymer-free SDS/water solution. This indicates that the surfactant is adsorbed and distributed over the polymer network and the fraction of hydrated SDS aggregates in the bulk is reduced. A time-induced viscosity enhancement is found for the HEC/SDS system at high SDS concentrations. An anomalous high viscosification (gel-like condition) of the HM-HEC/SDS system evolves over a long time at a high level of SDS addition.

(iv) These features for the HEC/SDS and HM-HEC/SDS systems are interpreted in the framework of a mechanism in which SDS hydrates are formed at low temperatures over time, and these clusters act as cross-linkers of the polymer network, leading to strengthening of the network and enhanced viscosity. The gel-like behavior observed for HM-HEC at high SDS concentration is attributed to the combined effect of cross-linkers and hydrophobic interactions.

(v) The SANS results demonstrate that the presence of polymer at high SDS concentrations and low temperatures has a stabilizing effect and hinders the formation of large crystals and precipitation of the surfactant. At the highest surfactant concentration (50 mM), the SANS results divulge a reorganization of the polymer network, and surfactant-induced clusters are proposed for the cross-linking of the network. In the absence of polymer, the SANS results at high levels of SDS addition and low temperature announce the formation of crystallites.

Acknowledgment. The financial support of the Norwegian Research Council through the project 177665/V30 is gratefully acknowledged.

References and Notes

- (1) *Polymer–Surfactant Systems*; Kwak, J. C., Ed.; Marcel Dekker: New York, 1998; Vol. 77.
- (2) Malmsten, M. *Surfactants and Polymers in Drug Delivery, Drugs and the Pharmaceutical Sciences*; Marcel Dekker: New York, 2002; Vol. 122.
- (3) *Surfactants and Polymers in Aqueous Solution*, 2nd ed.; Holmberg, K., Jönsson, B., Kronberg, B., Lindman, B., Eds.; John Wiley & Sons Ltd.: West Sussex, 2003.
- (4) Nyström, B.; Kjøniksen, A.-L.; Beheshti, N.; Zhu, K.; Knudsen, K. D. *Soft Matter* **2009**, 5, 1328.
- (5) Beheshti, N.; Nguyen, G. T. M.; Kjøniksen, A.-L.; Knudsen, K. D.; Nyström, B. *Colloid Surf., A* **2006**, 279, 40.

- (6) Miyajima, T.; Kitsuki, T.; Kita, K.; Kamitani, H.; Yamaki, K. US Patent 5,891,450, April 6, 1999.
- (7) Beheshti, N.; Bu, H.; Zhu, K.; Kjøniksen, A.-L.; Pamies, R.; Hernández Cifre, J. G.; de la Torre, J. G.; Nyström, B. *J. Phys. Chem. B* **2006**, *110*, 6601.
- (8) Maleki, A.; Kjøniksen, A.-L.; Nyström, B. *J. Phys. Chem. B* **2005**, *109*, 12329.
- (9) Kjøniksen, A.-L.; Laukkanen, A.; Galant, C.; Knudsen, K. D.; Tenhu, H.; Nyström, B. *Macromolecules* **2005**, *38*, 948.
- (10) Watanabe, K.; Imai, S.; Mori, Y. H. *Chem. Eng. Sci.* **2005**, *60*, 4846.
- (11) Shinoda, K.; Yamaguchi, N.; Carlsson, A. *J. Phys. Chem.* **1989**, *93*, 7216.
- (12) Kawai, T.; Kamio, H.; Kondo, T.; Kon-No, K. *J. Phys. Chem. B* **2005**, *109*, 4497.
- (13) Zhang, J. S.; Lee, S.; Lee, J. W. *J. Chem. Eng. Data* **2007**, *52*, 2480.
- (14) Zhang, J. S.; Lee, S.; Lee, J. W. *J. Colloid Interface Sci.* **2007**, *315*, 313.
- (15) Shinoda, K. *Colloidal Surfactants*; Academic Press: New York, 1963.
- (16) Weil, J. K.; Smith, F. S.; Stirton, A. J.; Bistline, R. G., Jr. *J. Am. Oil Chem. Soc.* **1963**, *40*, 538.
- (17) Nakayama, H.; Shinoda, K. *Bull. Chem. Soc. Jpn.* **1967**, *40*, 1797.
- (18) Lange, H.; Schwuger, M. J. *Kolloid Z. Z. Polym.* **1968**, *223*, 145.
- (19) Flockhart, B. D. *J. Colloid Interface Sci.* **1961**, *16*, 484.
- (20) Moroi, Y.; Matuura, R. *Bull. Chem. Soc. Jpn.* **1988**, *61*, 333.
- (21) Nyström, B.; Thuresson, K.; Lindman, B. *Langmuir* **1995**, *11*, 1994.
- (22) Bu, H.; Kjøniksen, A.-L.; Knudsen, K. D.; Nyström, B. *Langmuir* **2005**, *21*, 10923.
- (23) Schwuger, M. J.; Lange, H. *Chim. Phys. Appl. Prat. Ag. Surface, C. R. Congr. Int. Deterg.* **1969**, *2*, 955.
- (24) Bakshi, M. S.; Kaura, A.; Miller, J. D.; Paruchuri, V. K. *J. Colloid Interface Sci.* **2004**, *278*, 472.
- (25) Kjøniksen, A.-L.; Galant, C.; Knudsen, K. D.; Nguyen, G. T. M.; Nyström, B. *Biomacromolecules* **2005**, *6*, 3129.
- (26) Bu, H.; Naess, S. N.; Beheshti, N.; Zhu, K.; Knudsen, K. D.; Kjøniksen, A.-L.; Elgsaeter, A.; Nyström, B. *Langmuir* **2006**, *22*, 9023.
- (27) Georgalis, Y.; Schüler, J.; Umbach, P.; Saenger, W. *J. Am. Chem. Soc.* **1995**, *117*, 9314.
- (28) Frank, J.; Holzwarth, J. F.; Saenger, W. *Langmuir* **2002**, *18*, 5974.
- (29) Nyström, B.; Thuresson, K.; Lindman, B. *Langmuir* **1995**, *11*, 1994.
- (30) Thuresson, K.; Söderman, O.; Hansson, P.; Wang, G. *J. Phys. Chem.* **1996**, *100*, 4909.
- (31) Piculell, L.; Egermayer, M.; Sjöström, J. *Langmuir* **2003**, *19*, 3643.
- (32) Olsson, M.; Boström, G.; Karlson, L.; Piculell, L. *Langmuir* **2005**, *21*, 2743.
- (33) Glasstone, S.; Laidler, K. J.; Eyring, H. *The Theory of Rate Processes*; McGraw-Hill: New York, 1941.
- (34) Patel, S. P.; Patel, R. G.; Patel, V. S. *Int. J. Biol. Macromol.* **1987**, *9*, 314.
- (35) Badiger, M. V.; Lutz, A.; Wolf, B. A. *Polymer* **2000**, *41*, 1377.
- (36) Durand, A.; Dellacherie, E. *Biomacromolecules* **2006**, *7*, 958.
- (37) Xu, X.; Chen, P.; Zhang, L. *Biorheology* **2007**, *44*, 387.
- (38) Cathébras, N.; Collet, A.; Viguier, M.; Berret, J.-F. *Macromolecules* **1998**, *31*, 1305.
- (39) Tirtaatmadja, V.; Tam, K. C.; Jenkins, R. D. *Langmuir* **1999**, *15*, 7537.
- (40) Ng, W. K.; Tam, K. C.; Jenkins, R. D. *J. Rheol.* **2000**, *44*, 137.
- (41) Caputo, M. R.; Selb, J.; Candau, F. *Polymer* **2004**, *45*, 231.
- (42) Smith, L. A.; Duncan, A.; Thomson, G. B.; Roberts, K. J.; Machin, D.; McLeod, G. *J. Cryst. Growth* **2004**, *263*, 480.

JP100333F